



POLITECNICO DI TORINO
Repository ISTITUZIONALE

Development of single-stage and Doherty GaN-based hybrid RF power amplifiers for quasi-constant envelope and high PAPR wireless standards

Original

Development of single-stage and Doherty GaN-based hybrid RF power amplifiers for quasi-constant envelope and high PAPR wireless standards / Moreno Rubio, Jorge Julian; Fang, Jie; Quaglia, Roberto; Camarchia, Vittorio; Pirola, Marco; Ghione, Giovanni. - In: MICROWAVE AND OPTICAL TECHNOLOGY LETTERS. - ISSN 0895-2477. - STAMPA. - 54:1(2012), pp. 206-210. [10.1002/mop.26459]

Availability:

This version is available at: 11583/2458625 since:

Publisher:

Wiley Periodicals

Published

DOI:10.1002/mop.26459

Terms of use:

openAccess

This article is made available under terms and conditions as specified in the corresponding bibliographic description in the repository

Publisher copyright

IOP postprint/Author's Accepted Manuscript

"This is the accepted manuscript version of an article accepted for publication in MICROWAVE AND OPTICAL TECHNOLOGY LETTERS. IOP Publishing Ltd is not responsible for any errors or omissions in this version of the manuscript or any version derived from it. The Version of Record is available online at <http://dx.doi.org/10.1002/mop.26459>

(Article begins on next page)

Development of single-stage and Doherty GaN-based hybrid RF power amplifiers for quasi-constant envelope and high PAPR wireless standards

J. Moreno, Jie Fang, R. Quaglia, V. Camarchia, M. Pirola, G. Ghione

*Department of Electronics (DELEN), Politecnico di Torino,
Corso Duca degli Abruzzi, 24, 10129 Torino, Italy.*

Abstract

The paper describes the design, realization and characterization of a set of hybrid medium-power RF power amplifiers, based on a commercial packaged GaN HEMT and developed through a low-cost microstrip process. Two different design solutions suitable for wireless applications are presented: the first, intended for a constant-envelope modulation (with reference to the GSM standard), is a Class F amplifier exhibiting at 900 MHz an efficiency of 72 % with an output power of 37.5 dBm; the second, optimized for non-constant envelope signals with high dynamics (with reference to the UMTS WCDMA standard), is a Doherty amplifier showing, at 2.14 GHz, an efficiency higher than 40 % at 6 dB of output power back-off with a maximum output power of 40 dBm.

GaN, power amplifier, microstrip, wireless communications, Doherty

Corresponding author

Roberto Quaglia

Dep. of Electronics - Politecnico di Torino

C.so Duca degli Abruzzi 24

I-10129 Torino, Italy

tel. +39-011-5644219

fax +39-011-5644149

email roberto.quaglia@polito.it

1- INTRODUCTION

As well known, the need to reduce DC power consumption and the dissipation in RF transmitters makes the increase of the efficiency one of the most important Power Amplifier (PA) design issues, both for handsets and base-station applications. High-efficiency solutions derive from standard schemes such as the Class B [1] in its several variants, and are typically based today on more advanced solutions like the Class E [2], Class D [3], or Class F [4]. However, the optimum choice of the PA implementation in terms of efficiency should also take into account the signal Peak to Average Power Ratio (PAPR), that is mainly determined by the modulation format and therefore by the specific wireless standard.

In this work, we focus our attention on the design of medium-power basestation amplifiers having as a target two well-established wireless signal formats: a quasi-constant envelope modulation scheme working at 900 MHz (the GSM standard) and an advanced modulation schemes with larger PAPR typical of WCDMA applications, working at 2.14 GHz (the UMTS standard). Notice that with the GSM signal format the total PAPR deriving from the channel statistics in a multi-carrier medium-power amplifier is low (0 dB for a single carrier, 3dB for a multi-carrier), while in the same conditions it is higher for the UMTS standard (from 3 dB to more than 10 dB) [5][6].

For the PA implementation, we choose to exploit GaN-based devices. In fact, HEMT field-effect transistors based on the GaN technology [7][8][9] exhibit today very interesting performances for RF wireless applications, since they are able to overcome the well-known limitations of the Si-based LDMOS [10], today the dominant technology in basestation PAs. The devices exploited in the present study were GaN HEMTs grown on a Si substrate provided by Nitronex [11].

The choice of the PA topology and operating class was suggested by the following remarks. For the 900 MHz GSM application, single-stage PAs have been adopted, and a Class F topology has been selected (after comparison with a Class B topology realized with the same device and substrate), since, as expected from the theory, it exhibits better performances, both in terms of efficiency and maximum output power.

For the 2.14 GHz WCDMA application the situation is more complex, since the high PAPR leads to operation with a significant Output Back Off (OBO) implying a severe penalty in terms of efficiency with respect to its peak values achieved at maximum output power. Combined stages, able to properly shape the efficiency curve as a function of the instantaneous power level, are effective in handling UMTS signals with good average efficiency. The Doherty Power Amplifier (DPA) [1][12], with a high efficiency region extending several dBs in back-off, and a relatively simple topology, has been therefore selected for the UMTS 2.14 GHz PA design.

To address the choice of the DPA building blocks, we have designed, fabricated, and characterized a Class B and Class F PAs for the 2.14 GHz band. Measurements showed that the advantage that the Class F PA exhibits 900 MHz with respect to Class B, are almost completely lost at 2.14 GHz, due to the increased parasitic effects that play a crucial role in packaged devices. These considerations, combined to the simpler Class B implementation with respect to Class F, have driven our choice at 2.14 GHz toward a tuned load Class B as the main cell of the DPA (actually biased in deep Class AB for linearity improvement), while similar considerations suggest to adopt for the peak amplifier a classical Class C stage.

The paper is organized as follows: Section 2 provides an overview of the adopted design strategies. The prototyping of the different building blocks, and the description of the motivations that have led to the design of the final structures, together with the comparison between simulation and measurement results, are carried out in Section 3. Finally, some conclusions are drawn in Section 4.

2- DESIGN STRATEGY

The realized PAs are based on the NPTB00004 GaN HEMT fabricated by Nitronex inc. [11], a packaged device capable of 5 W output power at 28 V drain bias, and operative frequency range 1-6 GHz.

To identify the optimum PA solutions for the two applications under study (constant envelope GSM at 900 MHz, high PAPR WCDMA at 2.14 GHz), we focused on the evaluation of the selected Class B and Class F PA test structures, through simulation and experimental characterization.

A test board was arranged to characterize the bare device in DC, small and large signal condition, to assess the model accuracy, extract parasitics, and obtain other information useful to the design. Especially important is the role played by parasitics, emphasized by the package contributions, which seriously impact on the design of Class B, and even more Class F PAs. In fact, only an accurate knowledge of parasitics permits to precisely shift the reference planes from the externally accessible terminals to the intrinsic ones [13], and to this purpose they have been carefully identified through cold FET measurements [14].

The load at the fundamental frequency of the Class B amplifier has been selected accounting for characterizations [15][16] and simulation results, adopting different strategies for the real and imaginary part. As well known, the real part of the load admittance forces the simultaneous maximum swing of current and voltage at the HEMT drain terminal. To this end, the maximum safe bias [11] and knee drain voltage (28 V and 4 V respectively), together with the maximum drain current (0.9 A) have been identified through measurements, that are in turn confirmed by simulation. A value slightly above 50 Ω has been chosen for Class B load $R_{opt,B}$, while for the Class F PA, according to [12] and having in mind a low-order Class F implementation with 3rd harmonic control, the previous value has been increased by a factor 1.15 (the theoretical factor for ideal Class F is 1.27).

The imaginary part of the load admittance at the fundamental (in theory, the same for Class B and F PA), has been obtained again through CAD simulations and measurements, but with exchanged roles. In fact, the choice of the load susceptance was based on the simulated instantaneous load line at the intrinsic device terminals, while load pull measurements, and other power characterization data, have been then exploited to validate the solution derived from the simulations.

As already mentioned, a low-order harmonic termination strategy has been adopted, controlling only the second and third harmonics according to Class B and Class F theory. Namely, for Class B PA, the second and third harmonics, at the intrinsic reference planes i.e. across the voltage controlled current drain source, have been chosen as close as possible to the short condition [1], while for the Class F PA short and open circuits for the 2nd and 3rd harmonics, respectively, have been designed and synthesized.

The PAs output matching networks (OMN), realized following the scheme shown in Fig. 1, have been designed to load both stages with the optimal terminations at fundamental, second and third harmonics, and to supply the device drain bias current.

The input matching networks (IMN) have instead been designed by means of large signal scattering simulations, accounting for the device gate self-biasing, to optimize the input match when the device is driven in high power regime. In- and out-of-band oscillation issues have been accurately dealt with, and unconditional stability in a wide bias range has been enforced introducing RC parallel networks in series to the HEMT, combined with a resistor inserted in the DC gate path.

FIG 1 HERE

Fig. 1: Block scheme of the designed OMNs.

3- PROTOTYPING AND RESULTS

The matching networks of the proposed PAs have been designed in the Agilent ADS CAD, the simulation of the distributed microstrip parts have been carried out at circuit level, and verified with Electromagnetic simulations by the Momentum tool of ADS. Layouts have been fabricated on a RF35 substrate ($H = 760 \text{ um}$, $\epsilon_r = 3.5$), and some test structures including microstrip junctions, stubs, lines, and via holes have been inserted in the PCB to assess the accuracy of the passive library models. A recessed brass has been devised and realized, to enable IMN and OMN separate mounting and characterization, to simplify the system assembly, and to ensure good electrical and thermal contact with the microstrip PCB.

900 MHz PAs

The bias point has been chosen, for both stages, slightly above the pinch-off, therefore accepting, with respect to Class B, a slight efficiency reduction [1], but better linearity. In particular, the drain current has been set to around 5 mA (1% of device maximum current), for a drain voltage of 28 V. Both PA configurations adopted the same IMN, reported in Fig. 2 that has been optimized to reduce in large signal operation, at the operative frequency of 900 MHz, the difference between available and actual input power to less than 0.1 dB.

FIG 2 HERE

Fig. 2: Topology of the IMNs for the 900 MHz PAs. The stabilization network is effective both in band and out band.

The large signal characterization of the two stages showed for the Class B PA a 5.2 W of output power with a gain of 21 dB, and peak drain efficiency just above 60 % (see Fig. 3). For Class F module, an output power of 5.7 W, a power gain of 21 dB, together with a maximum drain efficiency of 72 % have been measured (Fig. 4). As expected from the theoretical and simulated behaviors, the experimental characterization confirms the Class

F superior performances with respect to a corresponding Class B design. A picture of the realized Class F amplifier is shown in Fig. 5.

FIG 3 HERE

Fig. 3: Single Tone measurement of the 900 MHz Class B PA. Output power (black solid line), gain (red line + diamonds), and drain efficiency (blue line+ squares).

FIG 4 HERE

Fig. 4: Single Tone measurement of the 900 MHz Class F PA. Output power (black solid line), gain (red line + diamonds), and drain efficiency (blue line+ squares).

FIG 5 HERE

Fig. 5: Picture of the realized 900MHz Class F PA.

2.14 GHz PA

While for constant envelope application at 900 MHz the single stage solution is satisfactory, the design constraints at 2.14 GHz WCDMA suggest the DPA architecture, whose block diagram is sketched in Fig. 6. This configuration allows a wider high-efficiency region that covers the power span typical of non-constant envelope input signals.

FIG 6 HERE

Fig. 6: Block Scheme of the two stages DPA, with the same device employed for Main and Peak amplifier.

The same PAs topologies studied at 900 MHz have been redesigned at 2.14 GHz to identify the best solution for the realization of the Main and Peak stages of the DPA. The Class B PA exhibited a maximum output power of 5.2 W, a gain of 15.5 dB and a drain efficiency of 47 % (Fig. 7), while, the Class F, showed an output power of 5.4 W, a gain of 15.5 dB and an efficiency of 52 % (Fig. 8).

FIG 7 HERE

Fig. 7: Single Tone measurement of 2.14 GHz Class B PA. Output power (black solid line), gain (red line + diamonds), and drain efficiency (blue line+ squares).

FIG 8 HERE

Fig. 8: Single Tone measurement of 2.14 GHz Class F PA. Output power (black solid line), gain (red line + diamonds), and drain efficiency (blue line+ squares).

From these results it is evident that the performance gap between Class F and B exploited at 900 MHz is reduced, probably due the increased parasitic effects at 2.14 GHz. Moreover, resonances appear around 4 GHz due to the package parasitics, that compromise the accuracy of their identification for frequencies above 2 GHz, therefore leading to incorrect harmonic termination, and thus to poor waveform shaping at the intrinsic device level.

These considerations suggested adopting the Class B design for the DPA development, accounting also for its better compactness, and simpler layout if compared with Class F configuration. Moreover, to increase linearity, the Main amplifier has been actually biased in a deep Class AB (efficiency similar to the Class B but higher linearity), while the Peak amplifier has been biased in Class C.

A preliminary theoretical analysis to estimate the optimum operational conditions in terms of loads, bias currents and input power division, has been carried out [12]. This analysis has been performed adopting a tuned load configuration for Main and Peak amplifiers, and considering a 6 dB Output Power Back-off (OBO) as the break-point of the Doherty region. The Doherty Main amplifier load has been modulated from 130 Ω in the low power region to 65 Ω at saturation. The resulting Doherty common node load R_L , and the characteristic impedance Z_0 of the quarter-wave line impedance inverter have been calculated respectively as $R_L \cong 30 \Omega$ and $Z_0 \cong 60 \Omega$.

The output network of the Doherty, compensating the parasitics and synthesizing the fundamental and harmonic termination provided by the preliminary analysis is shown in Fig. 9. The input power division has been achieved by an uneven branch line splitter designed and optimized through EM simulations.

FIG 9 HERE

Fig. 9: Detailed scheme of output network for the designed DPA. Where is not specified, the line impedance is of 50 Ω .

The DPA has been realized (see Fig. 10), and characterized. The maximum delivered power at 2.14 GHz resulted in excess of 10 W, with efficiency higher than 40 % in a 6 dB region of OBO (Fig. 11), and reaching its peak value of 52 % at an output power of 10.5 W. The drain efficiency of the designed 2.14 GHz PAs is shown for increasing OBO in Fig. 12. For low OBO the DPA has efficiency comparable to Class F, and slightly larger than Class B; this can be attributed to the fact that the overall efficiency of the amplifier is affected by the highly efficient Class C peak stage, that, on the other hand contributes to decrease the DPA gain. With large OBO, the DPA clearly shows the expected advantage over the single-stage (Class F and Class B) solutions, together with a larger power. Approaching the power saturation conditions (i.e. decreasing OBO), the DPA output power is twice as the one of the single stages, since in this condition DPAs behave, as expected from the theory, as two combined stage modules.

FIG 10 HERE

Fig. 10: Picture of the fabricated DPA.

FIG 11 HERE

Fig. 11: Single Tone measurement of 2.14 GHz DPA. Output power (black solid line), gain (red line + diamonds), and drain efficiency (blue line+ squares).

FIG 12 HERE

Fig. 12: Drain efficiency vs. OBO for the three PAs designed at 2.14 GHz. Class B PA (blue + circles), Class F PA (red + diamonds), DPA (black + stars).

4- CONCLUSIONS

Two PA solutions for medium power transmitters have been designed, implemented and characterized. The first amplifier at 900 MHz is tailored for constant envelope modulation (GSM), while the second is conceived for 2.14 GHz high PAPR UMTS signals. Class B and Class F implementations of single-ended power amplifiers have been compared in terms of simulations and measurements at both frequencies, and a Doherty combined architecture has been chosen at 2.14 GHz. Tab. 1 summarize the performances of the designed modules in terms of gain, output power and efficiency, both at saturation, and at 6 dB OBO. At 900MHz, for constant envelope signals, Class F PA exhibits better performances in terms of output power, and drain efficiency.

At 2.14 GHz, a Class B architecture has been chosen for the DPA Main (in fact deep AB) and Peak (in fact C) cells, since parasitics more critical behavior suggested to focus on this more standard implementation, also considering its simpler topology with respect to Class F.

PA	P _{OUT}	Power Gain	Efficiency	
			@ 0dB OBO	@ 6dB OBO
Class B, 900 MHz	37.2 dBm	21 dB	62 %	34 %
Class F, 900 MHz	37.6 dBm	21 dB	72 %	36 %
Class B, 2140 MHz	37.3 dBm	15.5 dB	47 %	27 %
Class F, 2140 MHz	37.6 dBm	15.5 dB	52 %	28 %
Doherty, 2140 MHz	40.2 dBm	9.2 dB	52 %	40 %

Tab. 1: Resume of the measurements on the designed PA

ACKNOWLEDGMENTS

Support of the projects PRIN 2007 M3ICGAN and of the NOE NEWCOM++ is kindly acknowledged.

REFERENCES

- [1] S. C. Cripps, "RF Power Amplifiers for Wireless Communications," Artech House, Inc., Norwood, 1999.
- [2] N.O. Sokal, A.D. Sokal, "Class E-A new Class of high-efficiency tuned single-ended switching power amplifiers," Solid-State Circuits, IEEE Journal of , vol.10, no.3, pp. 168- 176, Jun 1975.
- [3] S.-A. El-Hamamsy, "Design of high-efficiency RF Class-D power amplifier," Power Electronics, IEEE Transactions on , vol.9, no.3, pp.297-308, May 1994.
- [4] F. H. Raab, "Class-F power amplifiers with maximally flat waveforms," IEEE Trans. Microwave Theory Tech., vol. 45, pp. 2007–2012, Nov. 1997.
- [5] E.W. McCune, Jr., "Multi-mode and multi-band polar transmitter for GSM, NADC, and EDGE," Wireless Communications and Networking, vol.2, pp.812-815, 20 March 2003.
- [6] S. Hussain, Y. Louet, "Peak to Average Power Ratio Analysis of Multi-carrier and Multi-standard Signals in Software Radio Context," ICTTA 2008, pp.1-5, 7-11 April 2008.
- [7] J. Shealy, J. Smart, M. Poulton, R. Sadler, D. Grider, S. Gibb, B. Hosse, B. Sousa, D. Halchin, V. Steel, P. Garber, P. Wilkerson, B. Zaroff, J. Dick, T. Mercier, J. Bonaker, M. Hamilton, C. Greer, M. Isenhour, "Gallium nitride (GaN) HEMT's: progress and potential for commercial applications," GaAs IC Symposium, 24th Annual Technical Digest , pp. 243- 246, 2002.
- [8] S.C. Binari, W. Kruppa, H.B. Dietrich, G. Kelner, A.E. Wickenden, J.A. Freitas Jr, "Fabrication and characterization of GaN FETs," Solid-State Electronics, Vol. 41, Issue 10, pp. 1549-1554, October 1997.

- [9] V. Camarchia, S. Donati Guerrieri, M. Pirola, V. Teppati, A. Ferrero, G. Ghione, M. Peroni, P. Romanini, C. Lanzieri, S. Lavanga, A. Serino, E. Limiti, L. Mariucci, "Fabrication and nonlinear characterization of GaN HEMTs on SiC and sapphire for high-power applications," *International Journal of RF and Microwave Computer-Aided Engineering*, Volume 16, Issue 1, pp. 70–80, January 2006.
- [10] W. Pribble, J. Palmour, S. Sheppard, R. Smith, S. Allen, T. Smith, Z. Ring, J. Sumakeris, A. Saxler, and J. Milligan, "Applications of SiC MESFETs and GaN HEMTs in power amplifier design," in *IEEE MTT-S Int. Micro. Symp. Dig.*, vol. 3, 2002, pp. 1819–1822.
- [11] "NPTB00004 Datasheet", Nitronex Corporation, NDS-002 Rev. 2, Sep. 2008.
- [12] P. Colantonio, F. Giannini, E. Limiti, "High Efficiency RF and Microwave Solid State Power Amplifiers," John Wiley & Sons, Ltd, 2009.
- [13] Hyun-chul Park "High Efficiency Class F Amplifier Design in the presence of internal parasitic components of transistor," *Proceedings of the 36th European Microwave Conference*, pp. 184–187, September 2006.
- [14] Jing Lu, Yan Wang, Long Ma, Zhiping Yu, "A new small-signal modeling and extraction method in AlGaIn/GaN HEMTs," *Solid-State Electronics* Vol. 52 pp. 115–120, 2008.
- [15] M. Pirola, V. Teppati, V. Camarchia, "Microwave Measurements Part I: Linear Measurements," *IEEE Instrumentation & Measurement Magazine*, Vol. 10-2, pp. 14-19, 2007.
- [16] V. Camarchia, V. Teppati, S. Corbellini, M. Pirola, "Microwave Measurements. Part II – Nonlinear Measurements," *IEEE Instrumentation & Measurement Magazine*, Vol. 10-3, pp. 34-39, 2007.

FIGURES

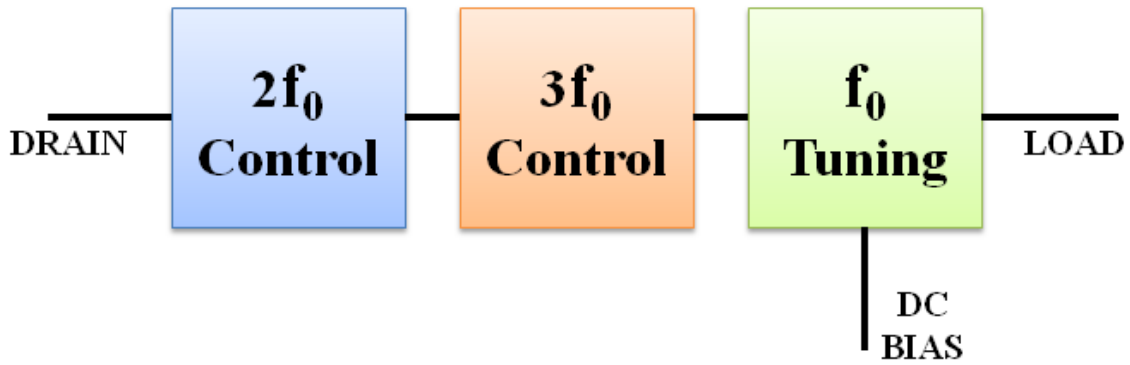


Fig. 13: Block scheme of the designed OMNs. The II harmonic is controlled just close to the drain, then III harmonic and fundamental are tuned

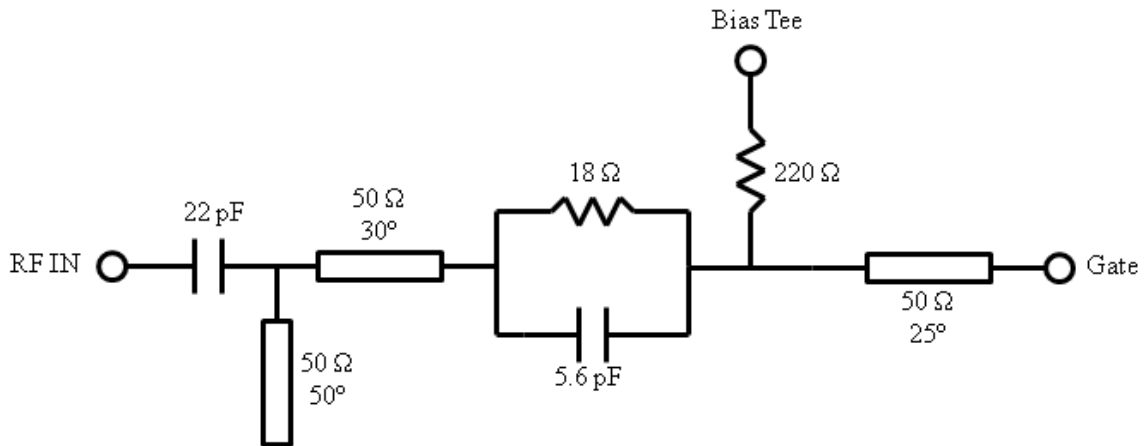


Fig. 14: Topology of the input matching network for 900 MHz PAs. The stabilization network is effective both in band and out band

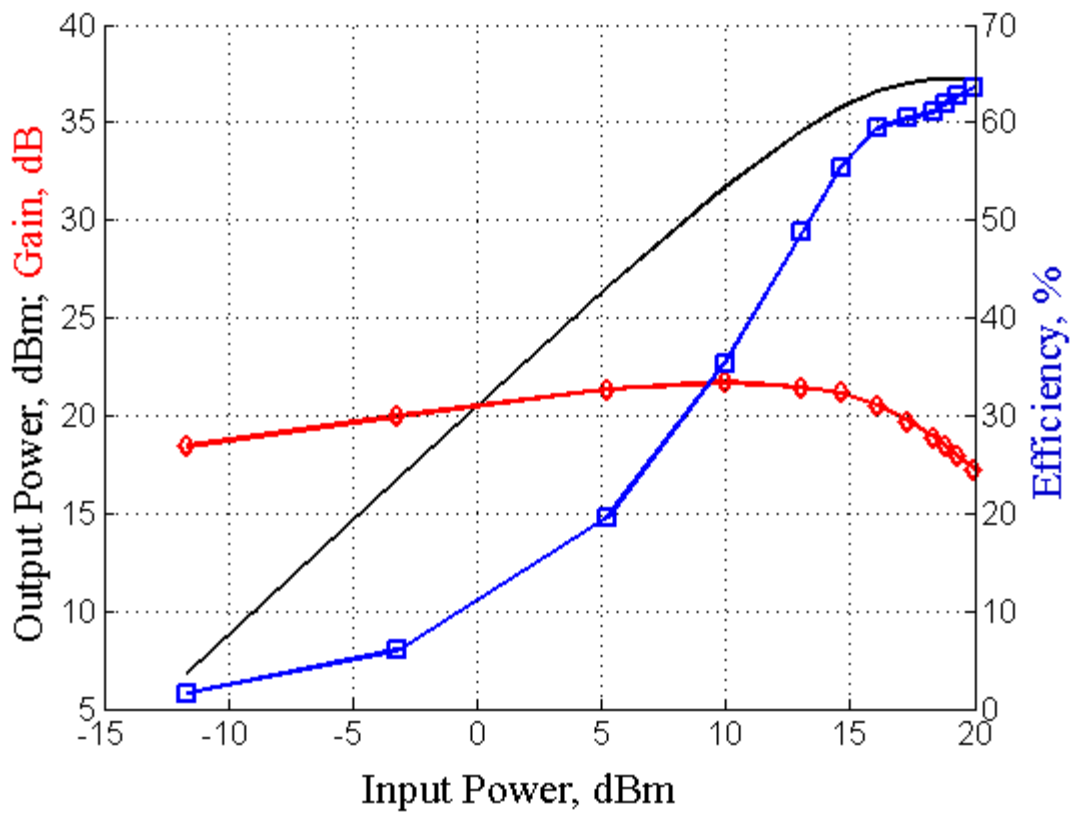


Fig. 15: Single Tone measurement of 900MHz Class B PA. Output power (black), operative gain (red + diamonds), efficiency (blue + squares)

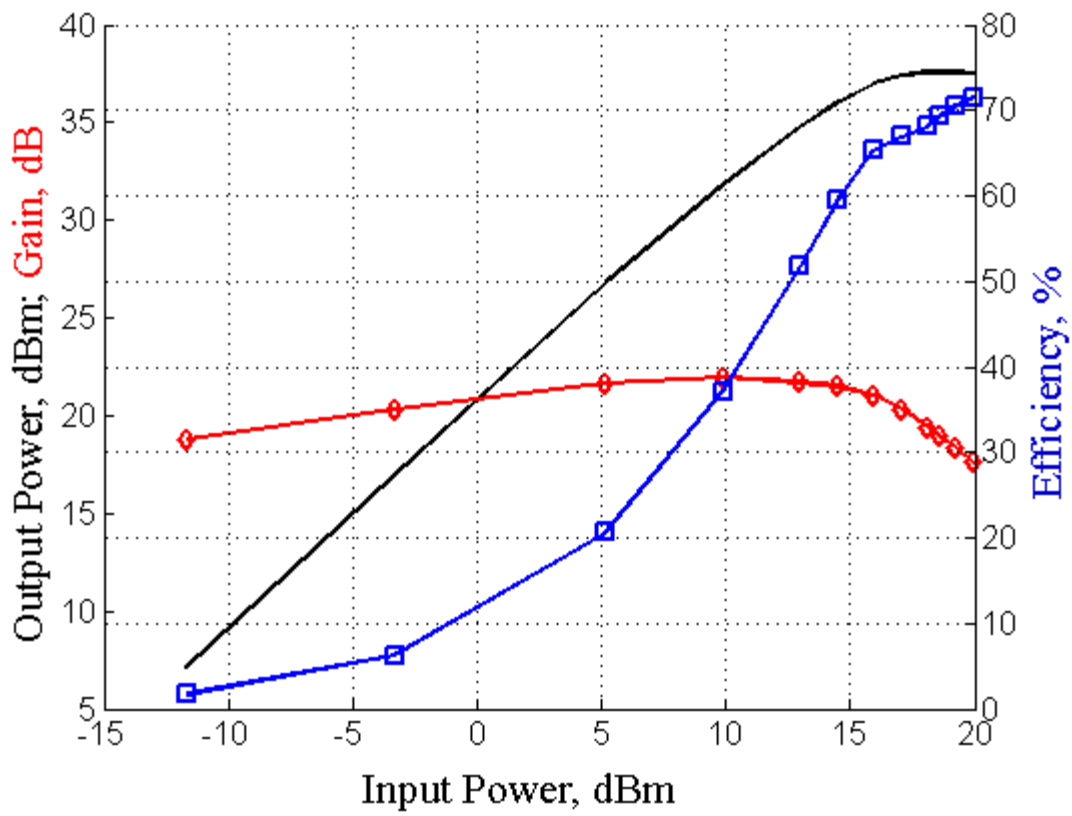


Fig. 16: Single Tone measurement of 900MHz Class F PA. Output power (black), operative gain (red + diamonds), efficiency (blue + squares)

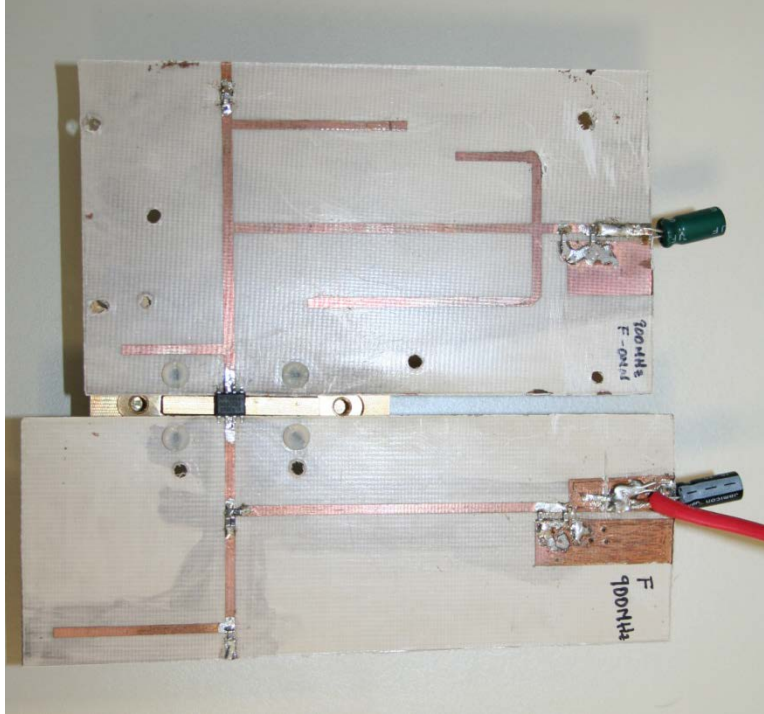


Fig. 17: Picture of the realized 900MHz Class F PA

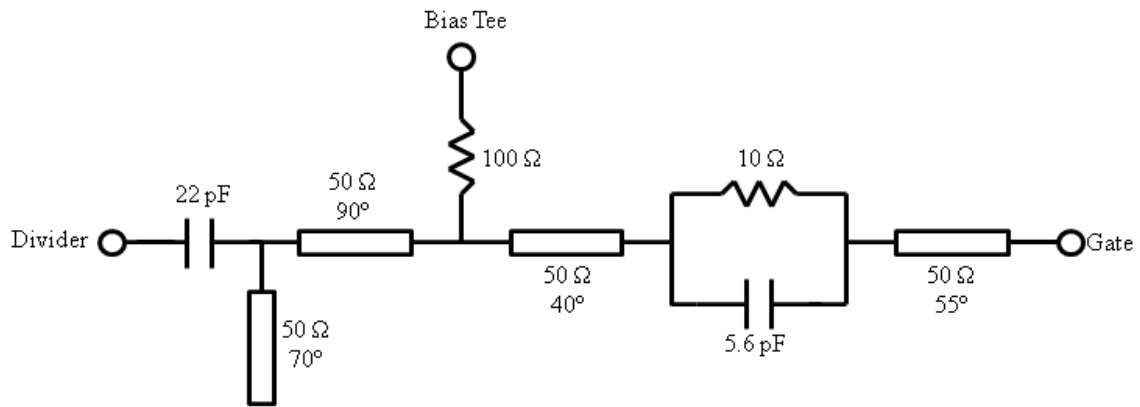


Fig. 18: Topology of the design IMN of the 2140 PAs. This network will be implemented also as IMN for Main and Peak amplifiers of the DPA

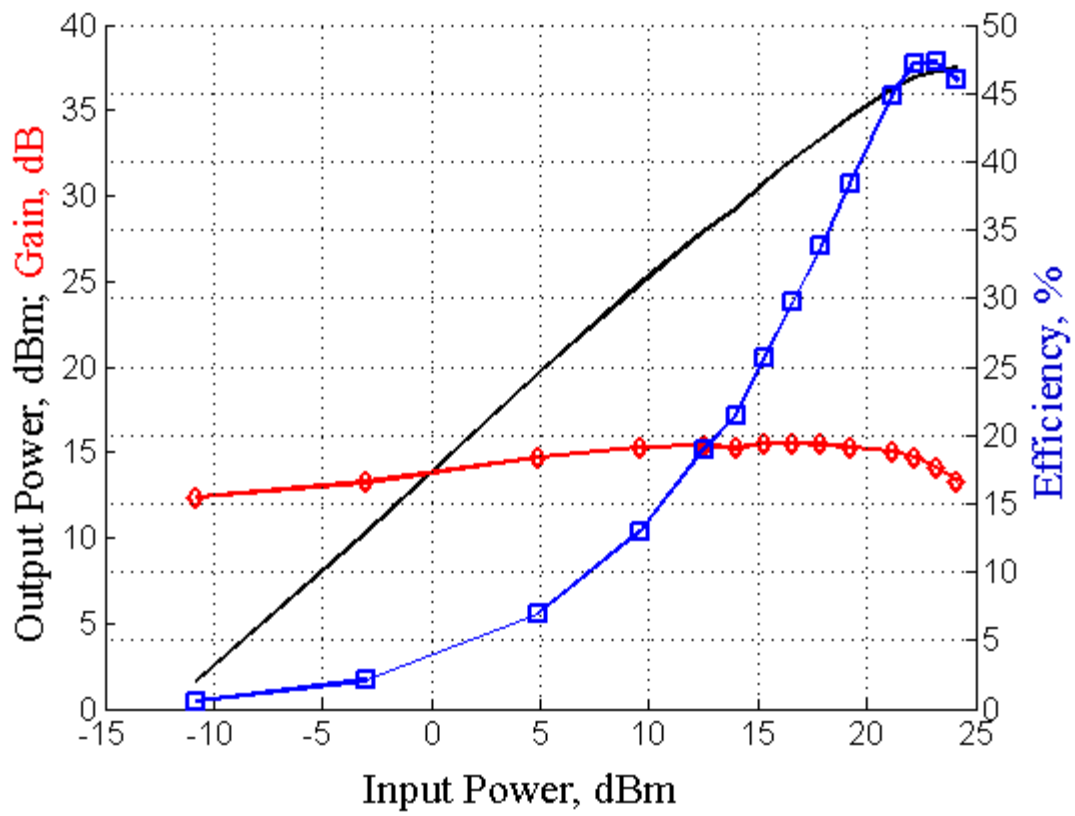


Fig. 19: Single Tone measurement of 2.14 GHz Class B PA. Output power (black), operative gain (red + diamonds), efficiency (blue + squares)

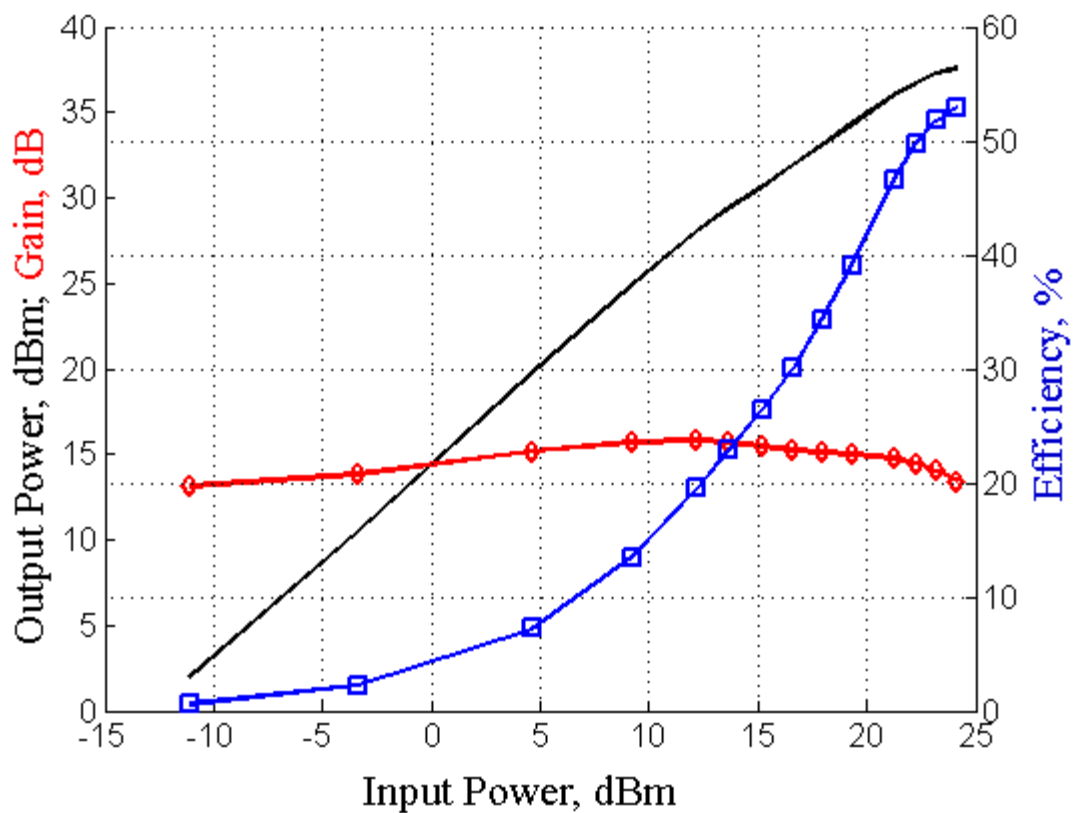


Fig. 20: Single Tone measurement of 2.14 GHz Class F PA. Output power (black), operative gain (red + diamonds), efficiency (blue + squares)

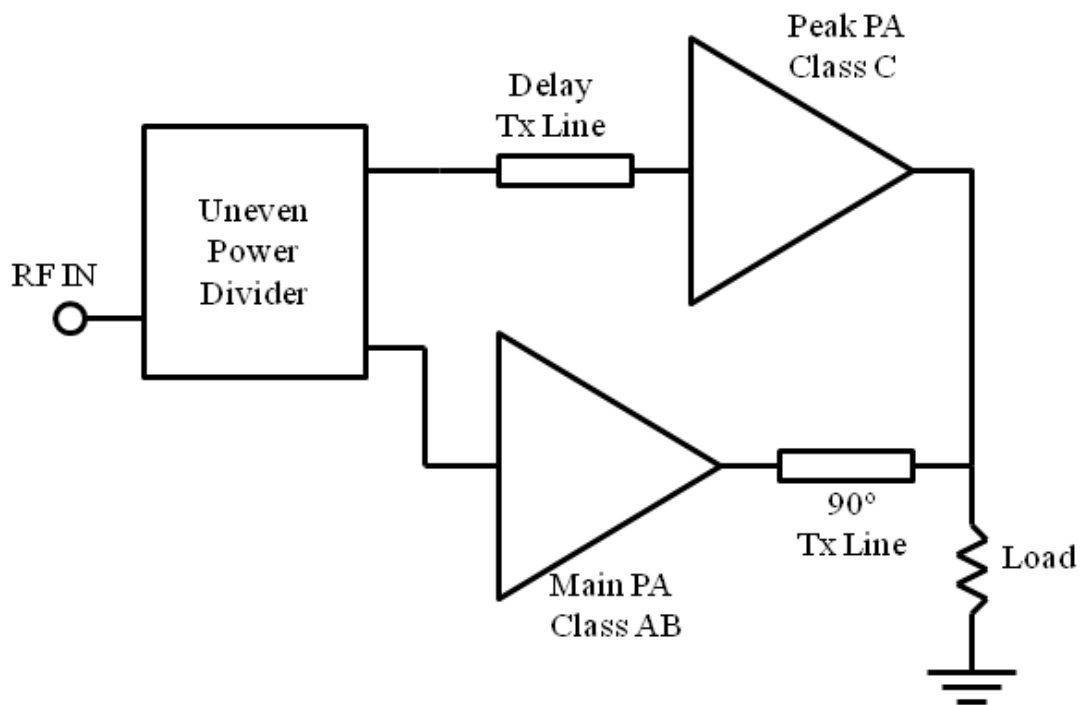


Fig. 21: Block Scheme of the two stage DPA, with the same device employed for Main and Peak amplifier

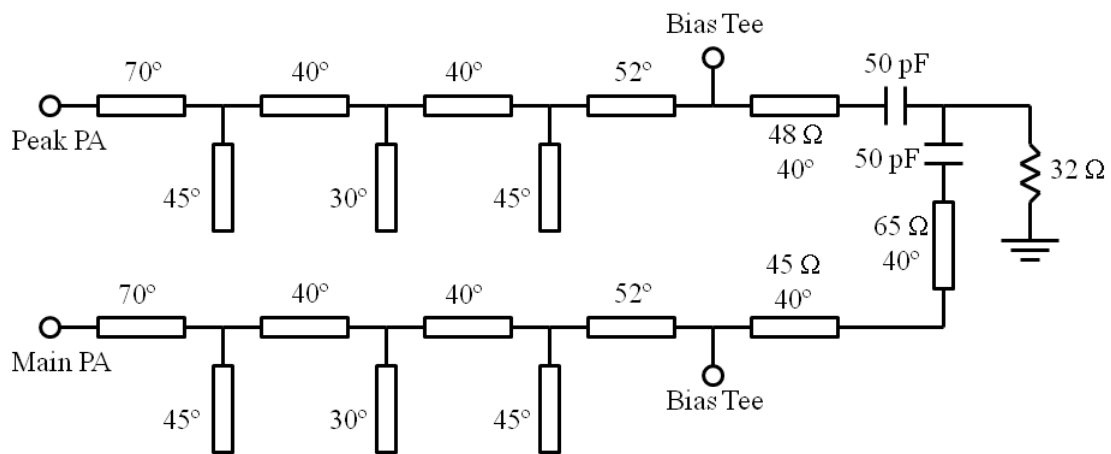


Fig. 22: Detailed scheme of output network for the designed DPA. Where is not specified, the line impedance is of 50 Ω .

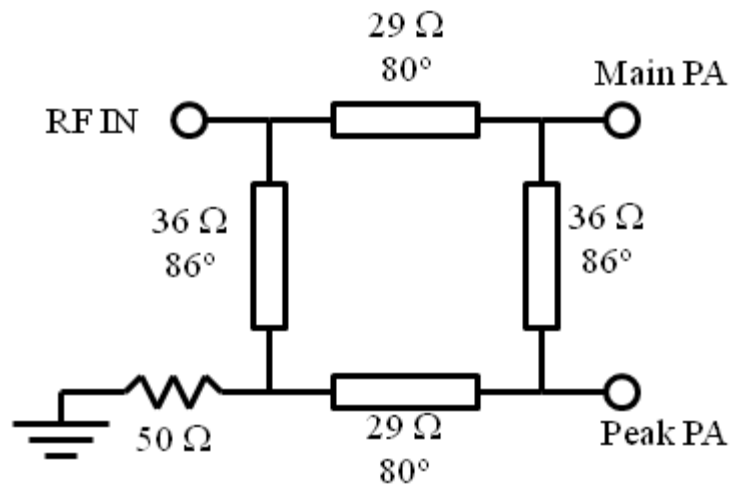


Fig. 23: Structure of the designed uneven branch-line splitter

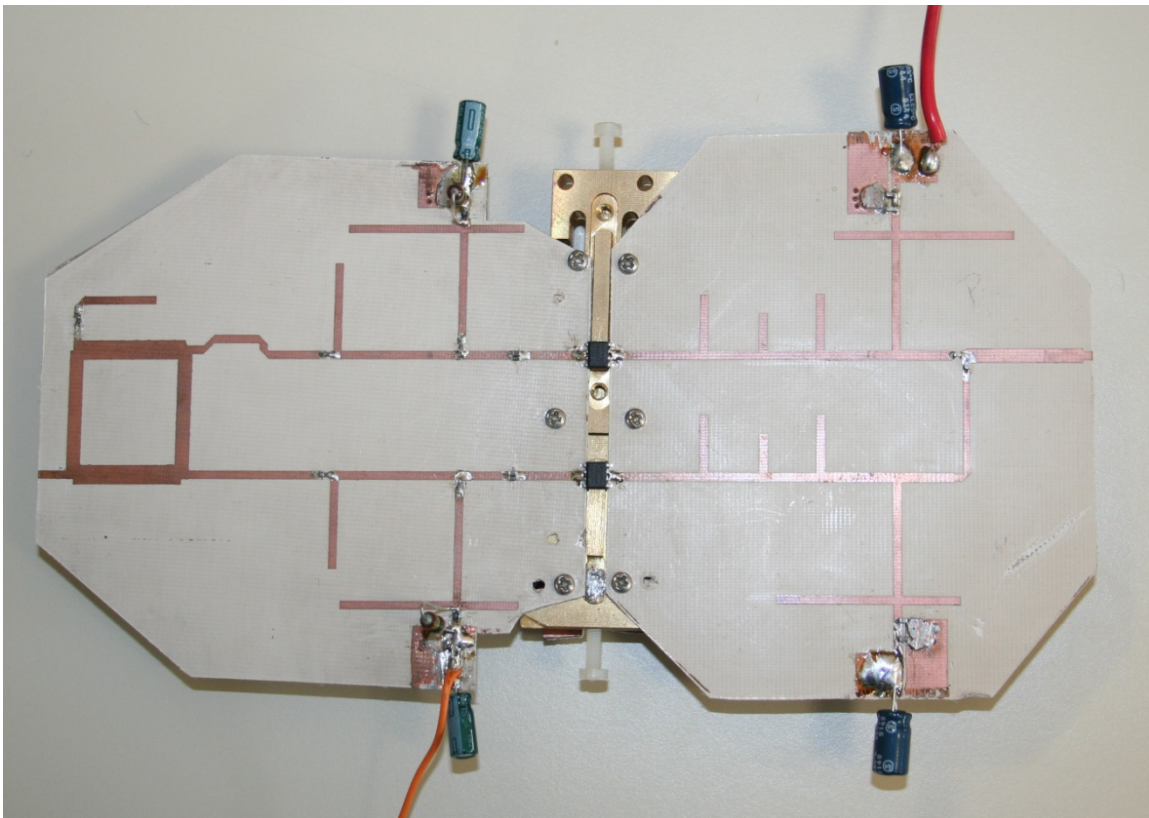


Fig. 24: Picture of the fabricated DPA

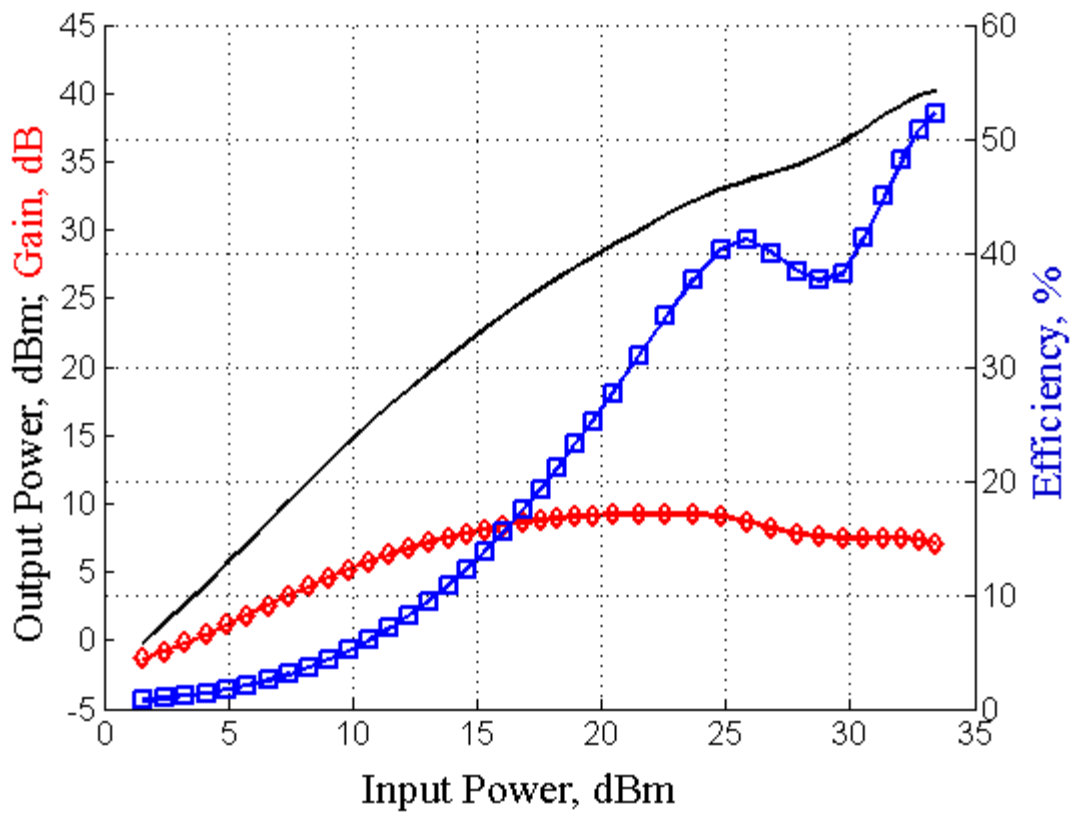


Fig. 25: Single Tone measurement of 2.14 GHz DPA. Output power (black), operative gain (red + diamonds), efficiency (blue + squares)